

Structure of Jupiter's upper atmosphere: Predictions for Galileo

Roger V. Yelle^{1,3}, Leslie A. Young¹, Ronald J. Vervack Jr.², Richard Young¹,
Leonard Pfister¹, and Bill R. Sandel²

¹Space Sciences Division, NASA Ames Research Center, Moffett Field, CA

²Lunar and Planetary Laboratory, University of Arizona, Tucson, AZ

Abstract. The Voyager mission to the outer solar system discovered that the thermospheres of all the giant planets are remarkably hot. To date, no convincing explanation for this phenomenon has been offered; however, there are a number of recent observational results which provide new information on the thermal structure of Jupiter's upper atmosphere that bear on this outstanding problem. We present an analysis of Jupiter's thermal structure using constraints from H_3^+ emissions, Voyager UVS occultation data, ground-based stellar occultation data, and the properties of the Jovian UV dayglow. Although the initial, separate analysis of these data sets produced contradictory results, our reanalysis shows that the observations are consistent and that the temperature profile in Jupiter's upper atmosphere is well constrained. We find that the data demand the presence of a large temperature gradient, of order 3-10 K/km, near a pressure of 0.3 μ bar. Analysis of the temperature profile implies that an energy source of roughly $1 \text{ erg cm}^{-2} \text{ s}^{-1}$ is required to produce the high thermospheric temperature and that this energy must be deposited in the 0.1-1.0 μ bar region. It is also necessary that this energy be deposited above the region where diffusive separation of CH_4 occurs, so that the energy is not radiated away by CH_4 . We show that dissipation of gravity waves can supply the energy required and that this energy will be deposited in the proper region. Moreover, because the turbulent mixing caused by gravity waves determines the level at which diffusive separation of CH_4 occurs, the location of the energy source (dissipation of waves) and the energy sink (radiation by CH_4) are coupled. We show that the gravity waves will deposit their energy several scale heights above the CH_4 layer; energy is carried downward by thermal conduction in the intervening region, causing the large temperature gradient. Thus dissipation of gravity waves appears to be a likely explanation for the high thermospheric temperature. Our arguments are general and should apply to Saturn, Uranus, and Neptune, as well as Jupiter. The model temperature profiles presented here and the relationship between the gravity wave flux and thermospheric temperature are directly testable by the Atmospheric Structure Instrument carried by the Galileo probe.

1. Introduction

Thermal models based on absorption of solar EUV radiation and thermal conduction, which work well for Earth, predict temperature rises in the thermospheres of the giant planets of the order of 10 K or less [Strobel and Smith, 1973]. The observed temperature rise in all of the giant planet atmospheres is many hundreds of kelvins [Atreya *et al.*, 1979; Broadfoot *et al.*, 1981; Smith *et al.*, 1983; Herbert *et al.*, 1987; Broadfoot *et al.*, 1989; Stevens *et al.*, 1992]. No convincing explanation for these large temperatures has been offered and it has remained an outstanding problem with our understanding of giant planet atmospheres.

The existence of high temperatures in the outer planet thermospheres is well established through a variety of measurements. The first hints of high thermospheric temperatures came from Pioneer measurements of the

electron temperature in Jupiter's ionosphere [Fjeldbo *et al.*, 1976], but the first estimates of the neutral thermospheric temperature were derived from Voyager UVS occultation measurements. On Jupiter, analysis of the UVS solar occultation implied a temperature of $1100 \pm 200 \text{ K}$ [Atreya *et al.*, 1979; Festou *et al.*, 1981; McConnell *et al.*, 1982]. Subsequent to this was the discovery of H_3^+ emissions from auroral and equatorial regions of Jupiter [Drossart *et al.*, 1989; Trafton *et al.*, 1989; Marten *et al.*, 1994]. The H_3^+ emissions are temperature dependent, and analysis of the vibrational and rotational structure implies temperatures of $800 \pm 100 \text{ K}$ in the equatorial regions [Marten *et al.*, 1994]. The H_3^+ emissions are formed in Jupiter's ionosphere at nanobar pressures or less

Although the existence of high thermospheric temperatures is well established, the characteristics of the temperature profile are not. The location of the thermospheric temperature gradient has been only poorly constrained. This circumstance has hampered investigations into the nature and identity of the energy source responsible for the high temperatures. We critically reexamine a variety of data on the Jovian thermosphere, including some recent results, and determine the range of temperature profiles consistent with the observations. We show that there is a strong temperature gradient, between 3 and 10 K/km, near 0.3 μ bar, just above the CH₄ homopause. We argue that these characteristics have strong implications for the energy source and suggest that dissipation of gravity waves is responsible. Based on this hypothesis, we make predictions testable by the Atmospheric Structure Instrument on the Galileo probe.

2. Summary of Observational Results

The solar occultation experiment performed by the Ultraviolet Spectrometer (UVS) on the Voyager 1 spacecraft measured the neutral atmospheric temperature directly and found $T=1100\pm 200$ K [Atreya *et al.* 1979; Festou *et al.*, 1981; McConnell *et al.*, 1982]. The solar occultation experiment measures atmospheric extinction caused by absorption in the ionization continuum of H₂, below 850 Å. The experiment is sensitive to line-of-sight column density of roughly 10^{17} cm⁻², which corresponds to a pressure level of $\sim 10^{-2}$ nbar; essentially, the solar occultation measures the exospheric temperature. Because the disc of the Sun, projected onto the Jovian atmosphere, subtended 800 km during the solar occultation, it was not possible to extract meaningful information from the lower thermosphere where the atmospheric scale heights are smaller.

The UVS on Voyager 2 observed an occultation of the star α -Leo by Jupiter. Analysis of these data is presented by Festou *et al.* [1981]. The stellar occultation measures atmospheric extinction at wavelengths from 911 to 1700 Å, although for this particular experiment the signal-to-noise level in the data is poor at the long-wavelength end of this range. Extinction from 911 to 1106 Å is due to absorption in the electronic bands of H₂ and absorption in the dissociation and ionization continua of several hydrocarbon species (CH₄, C₂H₂, and C₂H₆). Extinction from 1106 to 1700 Å is due exclusively to hydrocarbons. The measured extinction in the H₂ electronic bands can be analyzed to determine temperature, but detailed models are required because the absorption does not obey Beer's law and the occultation light curves do not directly reflect the scale height of the atmosphere. The Festou *et al.* analysis determined a temperature of 200 ± 30 K at a pressure of $1.0^{+1.0}_{-0.5}$ nbar and a temperature of 425 ± 25 K at a

pressure of 3×10^{-4} nbar. The validity of these results will be reviewed below. The α -Leo occultation occurred at a planetocentric latitude of 14.5°N.

The α -Leo occultation also determined the location of the CH₄ homopause on Jupiter. Extinction was measured in the 1282-1393 Å region, where H₂ is a very weak absorber. According to Festou *et al.* [1981] the observed light curves for this wavelength interval display a sharp drop in transmission at an altitude of 336 km above 1 bar, which corresponds to a pressure of 5 μ bar. Festou *et al.* argue that the extinction is due to a combination of absorption by CH₄ and C₂H₆ and estimate mixing ratios for these species of $2.5^{+2.0}_{-1.5}\times 10^{-9}$ and $2.5^{+2.0}_{-1.5}\times 10^{-9}$ at 5 μ bar.

The existence of high temperatures in Jupiter's upper atmosphere has been verified by observations of H₃⁺ emissions. These emissions were originally discovered in the Jovian auroral zones [Drossart *et al.*, 1989; Trafton *et al.*, 1989; Miller *et al.*, 1990], but the emissions are present at all latitudes [Marten *et al.*, 1994; S. Miller, personal communication, 1995]. Analysis of the rotational structure of the ν_2 band of H₃⁺ provides a good measure of the kinetic temperature in the line formation region. Marten *et al.* [1994] determine a temperature of 800 ± 100 K. Temperatures in the auroral regions appear to be higher [Drossart *et al.*, 1993]. The observations analyzed by Marten *et al.* were made of the North Equatorial Belt at about 10°N latitude in March 1992.

The H₃⁺ emissions themselves provide no information on the pressure regime where the lines are formed. However, ionospheric models predict that H₃⁺ should have a density profile that is peaked close to the electron density peak [McConnell and Majeed, 1987]. Radio occultation experiments were performed to determine the electron density profile during the Voyager 1 and 2 encounters [Eshleman *et al.*, 1979a, b]. The results for equatorial latitudes indicate that the peak occurs at an altitude of 1600-2300 km above 1 bar [Eshleman *et al.*, 1979a]. This information, coupled with atmospheric models to be presented in the following section, implies that the H₃⁺ emissions are produced at pressures less than 1 nbar.

At pressures of the order of 1 nbar the atmosphere should be close to isothermal and the 800 ± 100 K inferred from the H₃⁺ emissions should be the exospheric temperature. The 800 ± 100 K inferred from the H₃⁺ emissions is slightly lower than the 1100 ± 200 K inferred from the Voyager 1 solar occultation experiment, but the two determinations agree within the relative uncertainties. Of course, these observations were made more than one decade apart. In the discussions that follow we adopt 800 K as the exospheric temperature because the H₃⁺ observations were made at roughly the same time and at the same latitude as the other measurements to be discussed below.

On December 13, 1989, *Hubbard et al.* [1995] observed the occultation of the star SAO 78505 by Jupiter. By using an isothermal atmosphere model, they determined a temperature of 176 ± 12 K at a pressure of $1.8 \mu\text{bar}$, for a latitude of 8°N and an assumed half-light radius of 71880 km [*Hubbard and Van Flandern*, 1972]. This temperature was fairly consistent with those temperatures measured at similar latitudes from the occultation of β -Sco by Jupiter in 1971 [*Hubbard et al.*, 1972; *Veverka et al.*, 1974]. *Hubbard et al.* [1995] also performed an inversion of the SAO 78505 light curve and obtained results which agreed with the isothermal fits. However, *Hubbard et al.* [1995] used the results of *Festou et al.* [1981] to define the upper boundary condition. Because occultation inversion is sensitive to the upper boundary condition, we will show later that the SAO 78505 occultation does not rule out a steep thermal gradient at altitudes above $1 \mu\text{bar}$.

Recently, *Liu and Dalgarno* [1995] deduced a temperature of 500 - 600 K from analysis of H_2 emissions in the Jovian UV dayglow. They analyze spectra of the H_2 electronic band emissions obtained by the Hopkins

Ultraviolet Telescope (HUT) in late 1990 [*Feldman et al.*, 1993]. *Liu and Dalgarno* verify the suggestion by *Yelle et al.* [1987, 1988] that the Jovian UV dayglow is caused by a combination of fluorescence of sunlight in the H_2 electronic bands and photoelectron excitation. The interesting point for the thermal structure is that *Liu and Dalgarno* require a high temperature in order to reproduce the HUT spectra. The HUT spectral resolution is sufficient to reveal the rotational and vibrational structure of the H_2 emissions, which is determined by the temperature of the atmosphere. In order to analyze the HUT spectrum, *Liu and Dalgarno* calculate the UV dayglow spectrum assuming photoelectron excitation and solar fluorescence as the sources of the emissions. *Liu and Dalgarno* model the atmosphere as isothermal and adjust the temperature and column density of the atmosphere to find a best fit to the observations. They determine an atmospheric temperature of 500 - 600 K, with a best fit at 530 K, and a column density of $1 \times 10^{20} \text{ cm}^{-2}$. This column density corresponds to a pressure of $0.76 \mu\text{bar}$. An earlier version of the *Liu and Dalgarno* paper reported best fit

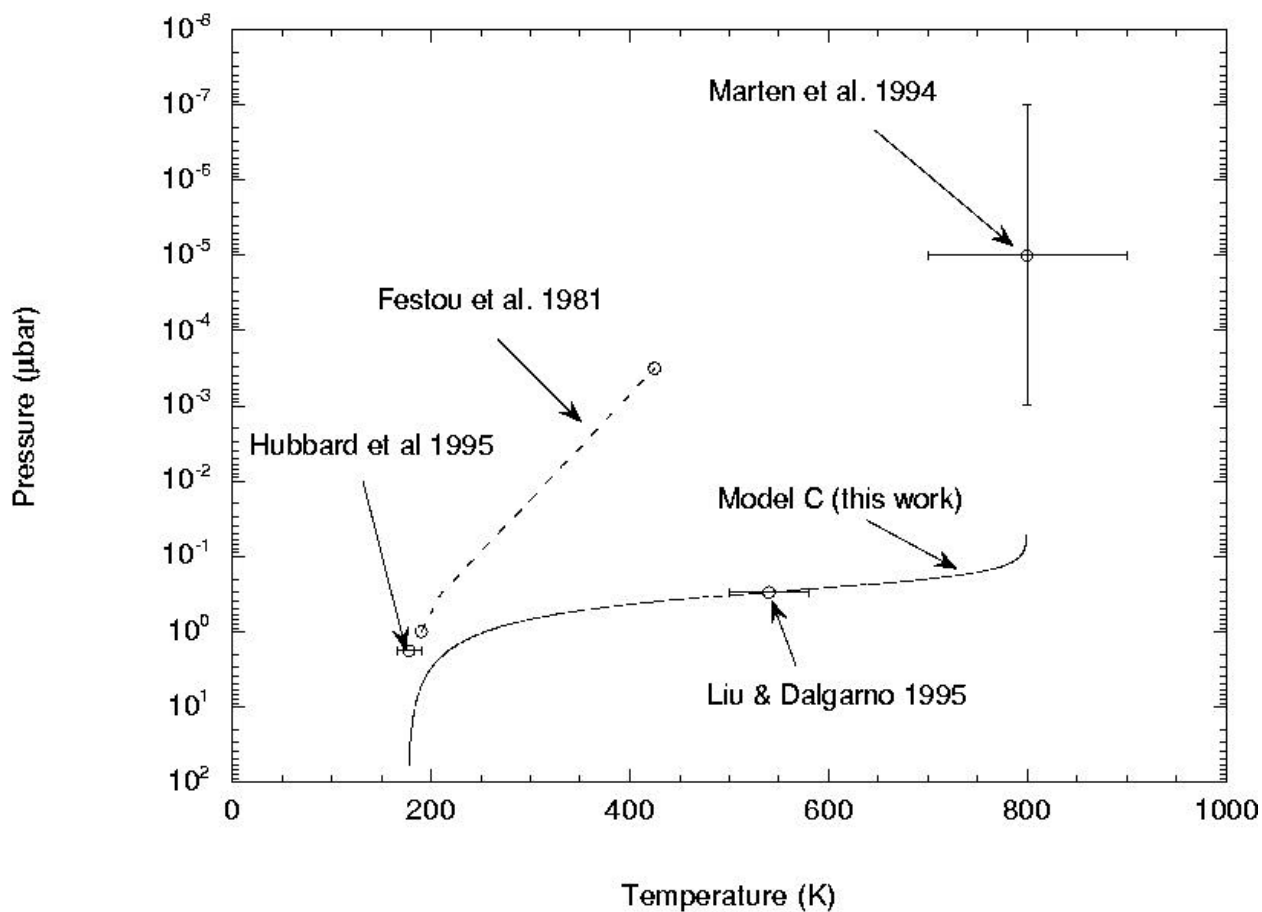


Figure 1. A summary of observational data on the thermal structure of Jupiter's upper atmosphere. The observations are discussed in the text. The solid curve represents an empirical temperature profile which we demonstrate to be consistent with all available measurements. The disagreement between the model proposed here and the model of *Festou et al.* [1981] is discussed further in the text.

values for temperature and column density of 540 K and $7 \times 10^{19} \text{ cm}^{-2}$ and these values are used in the analysis which follows. The temperature inferred by *Liu and Dalgarno* is an average for pressures less than 0.59 μ bar. If we model absorption in the atmosphere with the Curtis-Godson approximation, we conclude that 500-600 K represents the temperature at $\sim 0.3 \mu$ bar. The 500-600 K inferred by *Liu and Dalgarno* is much higher than the temperatures contained in the *Festou et al.* [1981] model at comparable pressure levels.

Figure 1 presents a summary of the observational data on the temperature of Jupiter's upper atmosphere. Clearly there are serious disagreements among results obtained from independent analysis of the various data sets. Not only is the *Liu and Dalgarno* [1995] temperature much higher than that contained in the *Festou et al.* [1981] model, but the *Hubbard et al.* [1995] temperature, which pertains to a pressure only slightly higher than *Liu and Dalgarno* [1995], is roughly 300 K lower. Also shown in Figure 1 is a temperature profile, derived below, which is consistent with the *Marten et al.* [1994] and *Liu and Dalgarno* [1995] analyses. In the next section we discuss the derivation of this temperature profile and demonstrate that it is consistent with the UVS α -Leo occultation and the SAO 78505 occultation as well as the *Liu and Dalgarno* [1995] and *Marten et al.* [1994] results.

3. The Temperature Profile

The inversion of occultation data depends sensitively on the choice made for the upper boundary condition. This problem has been well studied for groundbased refractive occultations [*Wasserman and Veverka*, 1973; *Hunten and Veverka*, 1976; *Baron*, 1989; *Rizk and Hunten*, 1990] but exists for absorptive occultations as well. Below, we demonstrate that the low temperatures retrieved by *Festou et al.* [1981] and *Hubbard et al.* [1995] are partly a reflection of choices made for the upper boundary condition and that both data sets are consistent with the presence of a large temperature gradient.

3.1 Temperature Gradient Models for the SAO 78505 Occultation

To analyze the SAO 78505 occultation, making use of the *Liu and Dalgarno* [1995] and *Marten et al.* [1994] results to define an upper boundary condition, we construct synthetic light curves based on an empirical temperature profile and compare the results to the light

curve for an isothermal atmosphere at a temperature of 176 K. We adopt a temperature profile of the form

$$T(z) = T_o + \frac{T_\infty - T_o}{1 + e^{-a|z-z_m|}}, \quad (1)$$

where z_m is the altitude of the maximum temperature gradient, T_o is the asymptotic temperature at high pressure, and T_∞ is the asymptotic temperature at low pressure. T_∞ is fixed at 800 K in all cases studied here. The parameter a is related to the maximum temperature gradient in the model and is given by

$$a = \frac{4}{T_\infty - T_o} \left. \frac{dT}{dz} \right|_{z=z_m} \quad (2)$$

The form of the temperature profile described by equation [1] has the virtue that it is isothermal at high and low altitudes and allows a large temperature gradient in the intervening region. Although the temperature gradients at pressures of a nonobar or less are much less than those near a microbar, the atmosphere does not necessarily become isothermal at high altitudes. The absorption of solar EUV radiation will heat the atmosphere by a small amount. However, the possibility of temperature gradients near a nanobar has no effect on our analysis, and nothing is lost by making the simple assumption that the atmosphere is isothermal in that region.

We search for temperature profiles which are consistent with the *Hubbard et al.* [1995] fit to the SAO 78505 data by specifying a maximum temperature gradient and scouring parameter space for values of T_o and z_m that give an adequate fit to the $T=176$ K light curve. We find that there is a range of values for the maximum temperature gradient for which it is possible to find combinations of T_o and z_m that fit the observations and present results for several cases below. In order to develop a criterion to judge the adequacy of the fit, we first calculate light curves for isothermal atmospheres at temperatures of 176, 164, and 188 K. These values correspond to the best fit, lower limit, and upper limits determined by *Hubbard et al.* [1995]. We then calculate the root mean square difference between the 176 K light curve and the 164 and 188 K light curves to estimate the noise level in the SAO 78505 data. A temperature gradient model is considered an acceptable fit if the root mean square difference from the 176 K isothermal model is less than the root mean square value for the 164 and 188 K isothermal models.

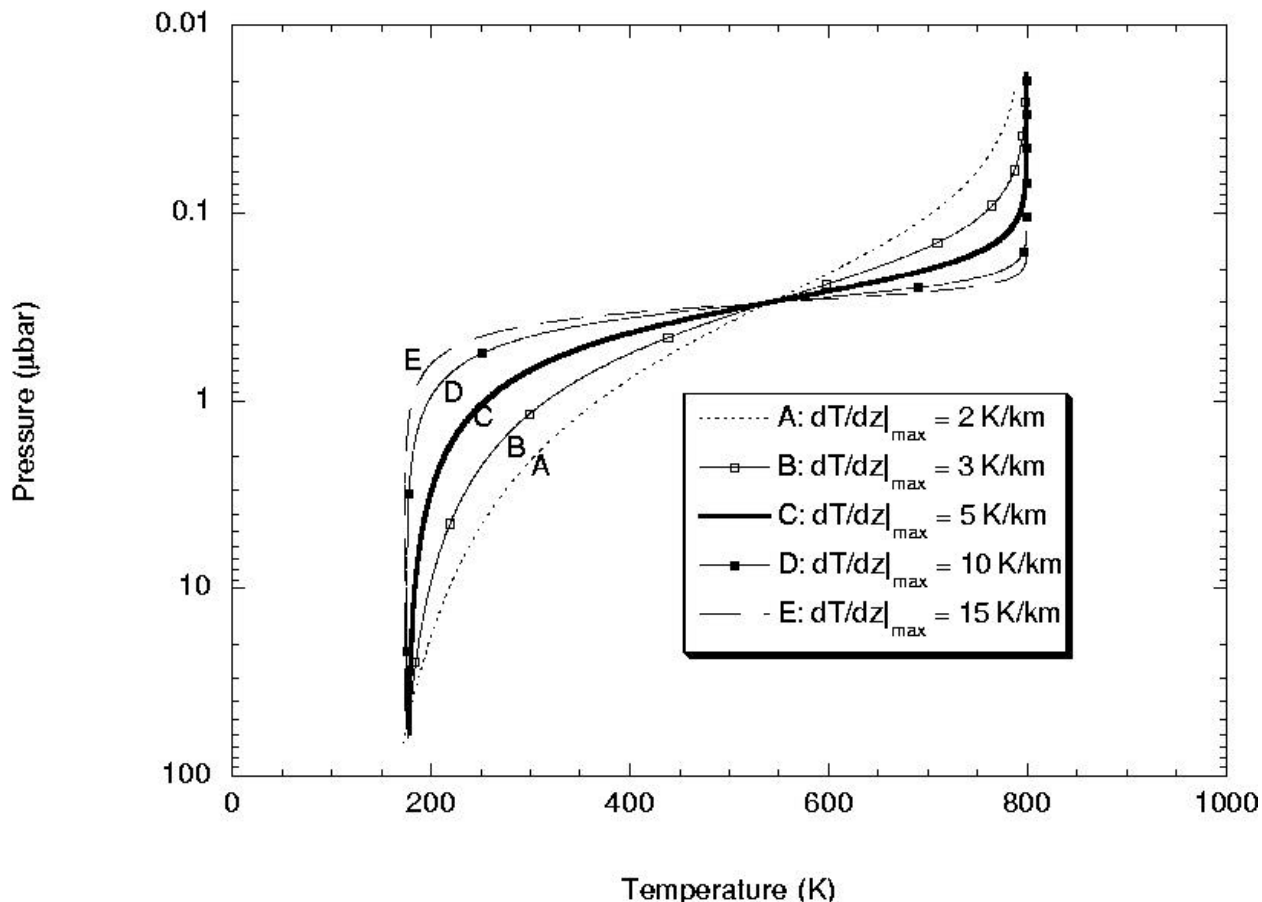


Figure 2. Model temperature profiles used in our reinterpretation of the SAO 78505 occultation observations. All the profiles are constrained to possess an exospheric temperature of 800 K and a temperature of 540 K at 0.3 μ bar. The profiles are characterized by different maximum temperature gradients, as indicated on the figure.

Figure 2 shows the temperature profiles for a range of maximum temperature gradients, while Figure 3 compares synthetic light curves based on these models with the light curve for an isothermal atmosphere at a temperature of 176 K. Model C provides an excellent fit, which is essentially indistinguishable from the isothermal light curve. Models B and D also provide acceptable fits. Models A and E are significantly worse. Thus we conclude that temperature profiles with large gradients are consistent with the SAO 78505 data and that the maximum temperature gradient lies between 3 and 10 K/km. It is worth noting that all the models have converged on an asymptotic temperature at high pressure near 176 K, as seen in Figure 2, and that the maximum temperature gradient occurs in the 0.3-0.5 μ bar region in every case.

It is possible that our procedure of fitting empirical, nonisothermal temperature models to Hubbard et al.'s isothermal fit to the SAO 78505 occultation may introduce artifacts into the analysis. If it were our intent to determine the temperature profile to high accuracy, this might be a problem; however, our purpose is to demonstrate that models with large temperature

gradients are consistent with the SAO 78505 occultation data and to obtain rough bounds on the size of permissible temperature gradients. Our procedure is adequate for this purpose. The differences between our suggested temperature profile and previous models is large, nearly 600 K at 0.2 μ bar. Any errors introduced by our procedure should be far smaller.

The temperature profiles proposed here are highly nonisothermal, whereas the *Liu and Dalgarno* [1995] analysis of the Jovian UV dayglow spectrum assumed an isothermal atmosphere. This may also introduce biases into our results. Without analyzing the UV dayglow spectrum with nonisothermal models (a formidable task which is outside the scope of this work) the nature and magnitude of this bias are difficult to assess; however, some information may be obtained by close examination of the *Liu and Dalgarno* calculations. In their Figure 6, *Liu and Dalgarno* show synthetic spectra for a column density of $1 \times 10^{20} \text{ cm}^{-2}$ and temperatures of 200, 530, and 1000 K. Spectral features near 111.5, 116.5, and 125.5 nm, caused by fluorescence of solar radiation, are most strongly affected by temperature. There are several features in the 130-

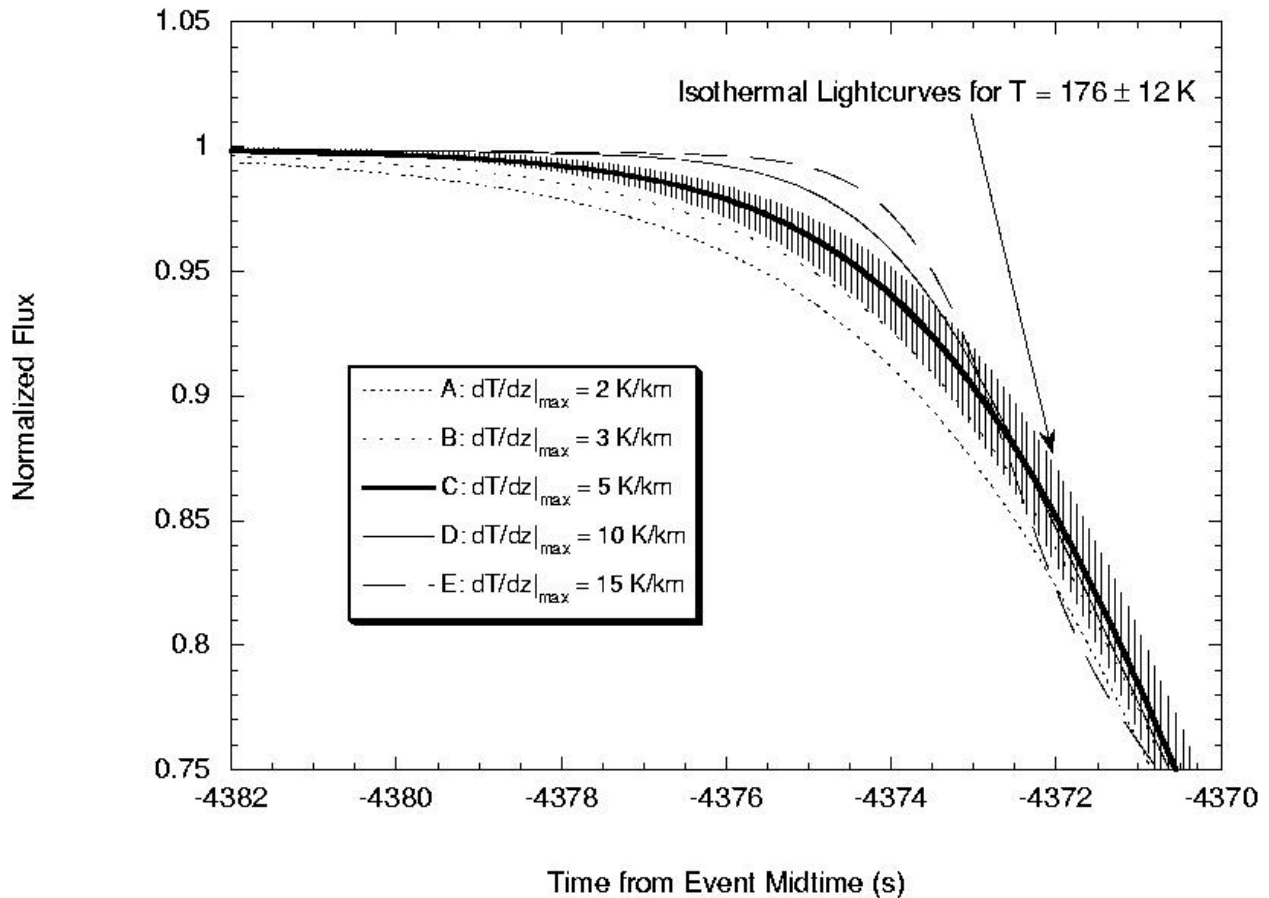


Figure 3. A comparison of synthetic light curves based on the models shown in Figure 2 and a synthetic light curve based on isothermal atmospheres with temperatures of 176 ± 12 K. The close agreement between model C and the $T=176$ K curve demonstrates that the large temperature gradient proposed here is a viable interpretation of the SAO 78505 data. Comparison of the temperature gradient models with the envelope defined by the uncertainty in the isothermal model implies that the maximum temperature gradient is constrained to lie between 3 and 10 K/km.

150 nm range which are caused by photoelectron excitation that are also temperature dependent, but their affect on the spectrum is small (see *Liu and Dalgarno* Figure 6). The excitation mechanism for the temperature dependent features is important because photoelectron excitation occurs at pressures of a nanobar or less, whereas excitation by solar fluorescence is concentrated near the base of the scattering column; thus emissions from these two mechanisms could be characterized by substantially different temperatures. Because the solar fluorescence features appear to dominate the temperature dependence, we tentatively conclude that the 0.3 μ bar inferred above for the location of the 540 K temperature point should be fairly accurate. We note however that a more sophisticated analysis of the UV dayglow spectrum, using a nonisothermal atmosphere, should result in lower temperatures at this pressure.

3.2 Reanalysis of the alpha Leo Occultation

In order to test whether the thermal profiles deduced above are consistent with the UVS data we have reanalyzed the α -Leo occultation data. There have been numerous improvements to the reduction and analysis techniques used for Voyager UVS occultation data since the Voyager Jupiter encounters. The reader is referred to *Yelle et al.* [1993] for a description of some of the improvements. Below, we discuss the essential aspects of the data reduction, present the results, and discuss the differences between our results and those of *Festou et al.* [1981].

The goal of the data reduction is to convert the spectra measured during the occultation into an accurate estimate of the atmospheric transmission. The first step in the data processing is to remove the signals caused by nonstellar sources from the spectra. *Festou et al.* [1981] identified three possible components to this background: (1) the interplanetary background, (2) emissions from the Jovian disk, and (3) the noise induced by energetic particles. In addition, there is a small component of noise introduced by the radioisotope thermoelectric

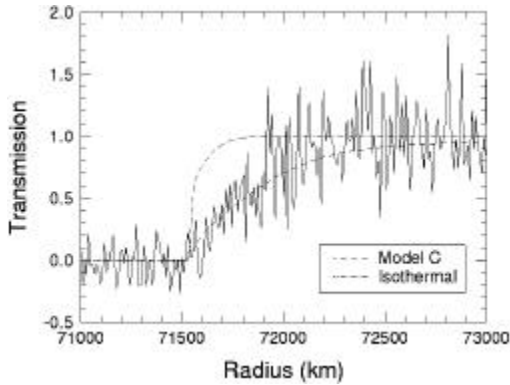


Figure 4. A comparison of synthetic light curves for the H_2 wavelength region based on model C and a $T=176$ K isothermal model with the UVS α -Leo occultation data. Models A-E produce essentially indistinguishable light curves. The good agreement between model C and the data implies that models with large temperature gradients are consistent with the UVS data.

generators on the spacecraft. We have carefully characterized the contribution of the nonstellar components and removed them from the spectra. What remains is a purely stellar signal modulated by the position of the star in the UVS slit and absorption by the Jovian atmosphere. The second step is to remove the effects of light scattered inside the instrument. *Festou et al.* claimed that this step is not necessary for the α -Leo data, but we have performed the removal to be completely thorough.

The third and final step is to divide each attenuated spectrum (I) by an unattenuated reference spectrum (I_o) taken with the star at the same position in the UVS slit. The position of the star in the UVS slit varies during an occultation because of spacecraft limit cycle motion (i.e., small variations in the spacecraft attitude). The stars position in the slit is important because it affects both the measured intensity and wavelength registration of the spectrum on the detector. These two effects can alter the shape of the I/I_o profiles if not properly taken into account. *Festou et al.* [1981] generated a single I_o spectrum by summing 200 spectra taken before the onset of absorption. spectrum by summing 200 spectra taken before the onset of absorption. They then multiplied all the spectra by a factor to account for the variation of intensity with slit position and divided by the I_o spectrum. They considered the spectral shift with the slit position negligible and made no correction for it. We bin the I_o spectra according to the position of the star in the slit. We then divide each I spectrum by the I_o spectrum that corresponds to the same position in the slit. This simultaneously accounts for the variation in intensity and the spectral shift caused by the motion of the star in the UVS slit. We have determined that the star moved roughly 0.0176 degrees during the attenuation period, causing a spectral shift of about 6 Å.

In the analysis which follows we limit ourselves to two wavelengths regions. The wavelength region from 1055 to 1083 Å is sensitive to both H_2 and hydrocarbon absorption, whereas wavelengths from 1285 to 1405 Å are sensitive to hydrocarbon absorption only. Because of the high noise level in these observations we are unable to obtain any reliable spectral information beyond that available from comparison of these two regions. The second wavelength region is chosen to completely avoid H_2 absorption, but further separation into regions primarily sensitive to CH_4 and C_2H_6 , as in the analysis of *Festou et al.* [1981] is not attempted. The hydrocarbon absorption is confined to relatively low altitudes compared with H_2 absorption, and using the 1285-1405 Å region, it is a simple matter to determine the altitude region over which the 1055-1083 Å region is affected by H_2 absorption only. In choosing the H_2 region, we have been careful to avoid potential stellar and interstellar medium absorption lines (Ly- β , etc.), whose presence would introduce large uncertainties into the analysis.

To determine if our model atmospheres, derived from the SAO 78505 observations, are consistent with the α -Leo data, we construct synthetic occultation light curves based on the model atmospheres and the absorption properties of H_2 and hydrocarbons. The method used to calculate H_2 absorption coefficients is described by *Yelle et al.* [1993]. Figure 4 shows a comparison of the α -Leo data with synthetic light curves generated using model C and an isothermal model at $T=176$ K. Clearly, the large temperature gradient model provides a better fit to the data than an isothermal model. In fact, it appears that nearly isothermal models are ruled out by the data. *Festou et al.* [1981] arrived at the same conclusion. Unfortunately, models A-E produce indistinguishable light curves (not shown in Figure 4); consequently, the UVS data can not be used to further constrain the temperature gradient beyond the information already obtained from the SAO 78505 occultation.

The pressure at which diffusive separation causes a rapid decrease in the CH_4 mole fraction is also a critical aspect of the atmospheric structure. To determine the location of the CH_4 homopause, we include CH_4 in the model atmospheres and construct synthetic light curves for comparison with the data from the hydrocarbon wavelength region. The CH_4 distribution is calculated by solving the usual transport equations for the transition from the heterosphere to homosphere [*Chamberlain and Hunten*, 1987; p. 93]:

$$D \left(\frac{1}{p_i} \frac{dp_i}{dz} + \frac{1}{H_i} \right) + K \left(\frac{1}{p_i} \frac{dp_i}{dz} + \frac{1}{H_a} \right) = \int_z^{\infty} J n_i dz', \quad (3)$$

where p_i is the CH_4 partial pressure, H_i is the CH_4 scale height in diffusive equilibrium, H_a is the atmospheric scale height, K is the eddy diffusion coefficient, and D is the molecular diffusion coefficient. The right-hand side of (3) represents loss due to photolysis of CH_4 . An eddy

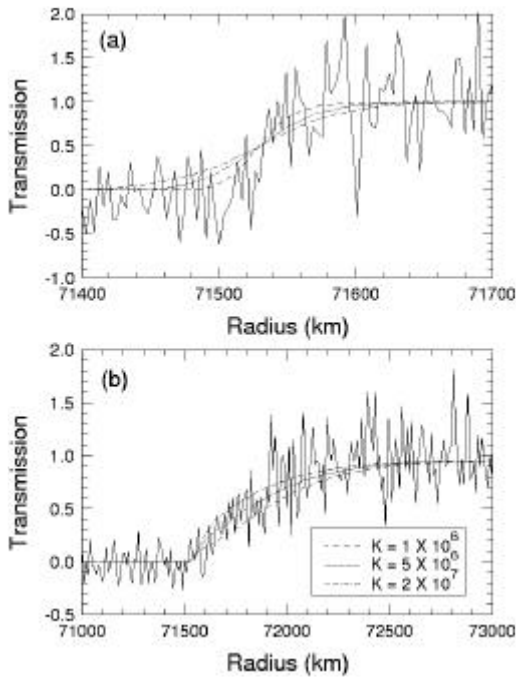


Figure 5. (a) A comparison of synthetic light curves for the hydrocarbon wavelength region with the UVS α -Leo occultation data. The synthetic light curves are based on model C and three different eddy diffusion coefficients, as indicated. The altitude scales for the models have been shifted to bring the half light points into agreement with the observations. (b) A comparison of synthetic light curves for the H_2 absorption region with the UVS α -Leo occultation data. These calculations are used to determine the pressure of the half-light level in the hydrocarbon wavelength region

diffusion coefficient which is constant with altitude is used in the calculations. The actual eddy diffusion coefficient is likely to be more complicated, but our goal here is simply to estimate the pressure level at which diffusive separation of CH_4 occurs and a constant eddy diffusion coefficient is sufficient for that purpose. A more physically based estimate of the eddy diffusion coefficient's altitude profile is presented in a later section.

A comparison of α -Leo data with synthetic light curves based upon model C and several different eddy diffusion coefficients is shown in Figures 5a and 5b. The sharp drop in the transmission in Figure 5a is caused by diffusive separation of CH_4 . Near the homopause, CH_4 begins to decrease with increasing altitude with a scale height determined by its own molecular mass. This scale height is roughly a factor of eight smaller than the atmospheric scale height; consequently, the transition appears abrupt. Changing the eddy diffusion coefficient alters the pressure at which diffusive separation occurs. Because the half light level in the hydrocarbon region is easily located, we shift the

altitude scale in the models to produce a match between synthetic and observed light curves for this region. This leaves an offset between the data and models in the H_2 light curves, as shown in Figure 5b. The results are shown for eddy diffusion coefficients of 5×10^6 , 1×10^6 , and $2 \times 10^7 \text{ cm}^2 \text{ s}^{-1}$; the latter values bracket the range of acceptable fits for the H_2 channels. This range for the eddy diffusion coefficient is consistent with the value of $K = 2_{-1}^{+6} \times 10^6 \text{ cm}^2 \text{ s}^{-1}$ derived by *Vervack et al.* [1995] from analysis of the He 584 Å dayglow, and the value of $K = 1.4_{-0.7}^{+0.9} \times 10^6 \text{ cm}^2 \text{ s}^{-1}$ derived by *Festou et al.* [1981].

Our determination of the CH_4 profile agrees well with that of *Liu and Dalgarno* [1995]. From the measured half-light points for the hydrocarbon channel and the thermal structure models we estimate that tangential optical depth unity for CH_4 absorption occurs at a pressure of $0.2_{-0.1}^{+0.6} \text{ mbar}$. The CH_4 mole fraction at the half-light level is $1 - 2 \times 10^{-4}$. We have assumed a CH_4 mole fraction of 2×10^{-3} in the lower atmosphere. The base of *Liu and Dalgarno's* atmosphere is determined by the location of the level for vertical optical depth unity for CH_4 absorption. The level of vertical optical depth unity for CH_4 absorption occurs at a pressure roughly a factor of 2 higher than the pressure for tangential optical depth unity; thus our results are consistent with the $0.6 \mu\text{bar}$ inferred by *Liu and Dalgarno* [1995] as the base of their H_2 scattering column. The pressure levels for vertical and tangential unit optical depth in CH_4 absorption lie close to one another because the CH_4 density is decreasing at a rapid rate relative to H_2 in the $0.2\text{-}0.6 \mu\text{bar}$ region. It is in this same pressure region that the temperature begins to rise rapidly. This feature of the atmospheric structure has important implications and is discussed in section 4.

The radius scale for the α -Leo occultation is determined from the spacecraft trajectory (supplied by the Jet Propulsion Laboratory), the position of Jupiter, and the location of α -Leo. Geometrical considerations give the distance from the center of Jupiter and latitude of the point of closest approach along the line of sight. We assume that the shape of Jupiter can be approximated by an oblate spheroid with an oblateness of 0.0649 for this calculation. Calculations done assuming a spherical shape yield results differing by less than 1 km and 0.05° from those for an oblate spheroid. This leads us to believe that if the calculations were done with the actual shape of Jupiter (which is not an oblate spheroid), the results would not be significantly different. The altitude scale is determined by subtracting the true radius of Jupiter at the occultation latitude of 14.5°N and 1 bar level (obtained from *Lindal et al.* [1981]) from the distance of closest approach. This procedure yields altitudes above the 1 bar level for the H_2 and hydrocarbon transmission profile half light points of 692_{-50}^{+46} and 459_{-10}^{+16} km, respectively. These values correspond to equatorial radii of 72184_{-50}^{+46} and 71951_{-10}^{+16} km. According to model C, the H_2 half-light

point occurs at a pressure of 2.5×10^{-6} mbar. Extrapolating to higher pressures using model C, we find the 1-mbar altitude to be 105_{-50}^{+76} km, which is consistent with the 1-mbar altitude of 160 km determined by *Lindal et al.* [1981].

Our results differ substantially from those of *Festou et al.* [1981]. The temperature gradient in those models is 0.55-0.65 K/km, which is significantly smaller than the temperature gradient determined by our analysis. We use slightly different wavelength ranges, new absorption coefficients for H_2 , and a different approach to the data reduction and analysis, but the differences caused by these improvements, developed over many years of UVS occultation data analysis, are small compared with the relatively large noise level in the data. The large differences between our results and those of *Festou et al.* [1981] are caused not by differences in data reduction or analysis procedures but by different assumptions about the upper boundary condition. *Festou et al.* considered nonisothermal atmospheres, but they assumed that the temperature gradient was mild. Lacking other information, they assumed that the maximum temperature was reached at an altitude greater than 1140 km above the 1 bar level, in order to connect the α -Leo results with the UVS solar occultation results at higher altitudes. *Festou et al.* clearly state that their results are contingent upon this assumption. Our temperature profile, which is driven by the *Liu and Dalgarno* results, violates this assumption. Thus the difference between our results and *Festou et al.* [1981] appears to be primarily related to assumptions about the upper boundary conditions, rather than any fundamental difference in approach.

4. Characteristics of the Energy source

We have demonstrated that the atmospheric temperature rises just as CH_4 begins to disappear. This is probably not a coincidence: CH_4 is an efficient radiator that plays a primary role in the thermal balance of the Jovian stratosphere [*Wallace, 1976*]. When CH_4 is present the heating source has a minor effect on the temperature because the extra energy is radiated away, but as the CH_4 density decreases because of diffusive separation and photolysis, the atmosphere can no longer cool efficiently and the temperature rises rapidly. Moreover, the energy source must extend for a significant distance above the level where CH_4 cools, because a separation between the heating source and sink is required to produce a large temperature gradient.

Above the level where the CH_4 abundance is appreciable, energy is carried by thermal conduction, and the energy flux, F , is given by $F = -\kappa \frac{dT}{dz}$, where κ is the thermal conductivity. Thus the energy flux is proportional to the maximum temperature gradient. Using $\kappa = AT^s$, where $A = 252 \text{ erg cm}^{-1} \text{ s}^{-1} \text{ K}^{-s}$ and $s = 0.751$ [*Hanley et al., 1970*], we find that models B, C, and D, with maximum temperature gradients of

3-10 K/km, correspond to energy fluxes of $0.8\text{-}2.8 \text{ erg cm}^{-2} \text{ s}^{-1}$. We conclude that the energy source responsible for the high thermospheric temperature must have a strength of approximately $1 \text{ erg cm}^{-2} \text{ s}^{-1}$.

In a steady state, the loss of energy by downward conduction is balanced by a heat source $Q = dF/dz$, which peaks at 0.15, 0.20, and 0.24 μbar for our empirical models B, C, and D. The pressure level at which energy is deposited does not depend strongly on the particular analytic form we use for the temperature profile in our models. To demonstrate this, we consider two extreme cases for the heat source: one in which energy is deposited in an infinitely thin layer [i.e. a delta function], and a more distributed case in which Q is proportional to density. In what follows, the temperature, pressure, scale height, and temperature scale height at the base of the constant-flux region to be $T_b = 540 \text{ K}$, $p_b = 0.3 \mu\text{bar}$, $H_b = 30 \text{ km}$, and $HT = [1/T \frac{dT}{dz}]^{-1} = 54\text{-}180 \text{ km}$, where the range reflects the uncertainty in the temperature gradient at 0.3 μbar .

The temperature profile for a delta function heat source is determined by solving the thermal conduction equation with a constant downward flux, $F = -\kappa T/H_T$. We assume that the energy is deposited at a pressure p_j . Then, at any pressure $p_j > p > p_b$ the temperature is given by

$$T^s = T_b^s \left(1 - \frac{sH_b}{H_T} \ln \left(p / p_b \right) \right). \quad (4)$$

For this model the atmosphere is isothermal at altitudes above p_j but increases monotonically at altitudes below p_j . Raising the altitude of the heat source (i.e., lowering p_j) results in larger asymptotic temperatures. Solving (4) for the pressure at which $T = 800 \text{ K}$ implies that $p_j = 0.13 \mu\text{bar}$ for model B and $0.23 \mu\text{bar}$ for model D.

For the model with Q proportional to density, the thermal conduction equation has the solution

$$T^s = T_b^s \left(1 + \frac{sH_b}{H_T} \right) \left(1 - p / p_b \right). \quad (5)$$

which is valid for all pressures. In order to determine if this distributed heat source is consistent with our temperature models we set $p = 0$ and solve equation (5) to determine the asymptotic temperature at low pressure. The results are $T = 850, 1080, \text{ and } 1700 \text{ K}$ for models B, C, and D. Temperatures of 850 and 1080 K are consistent with the available data; thus a heating rate proportional to density is consistent with models B and C. In all cases, 2/3 of the energy flux is deposited below 0.1 μbar .

It is worth emphasizing that the characteristics of the energy source implied by our derived temperature profile are profoundly different from those derived from the *Festou et al.* [1981] models. The maximum heating rate occurs essentially where the second derivative of temperature with respect to altitude has a maximum. Examination of the *Festou et al.* [1981, Figure 7] model reveals that this occurs near 1500 km, where the pressure is 10^{-2} nbar. Our maximum heating rate occurs

roughly at a pressure 4 orders of magnitude higher. The 10^{-2} nbar pressure level is essentially in the exosphere and much of prior speculation on the identity of the energy source for the outer planet thermospheres has centered around possible magnetospheric interactions and plasma processes in the ionosphere. *Hunten and Dessler* [1977] suggested that the precipitation of low energy electrons from the Jovian magnetosphere could be responsible for the high temperature. *Shemansky* [1985] postulated the existence of an anomalous distribution of low-energy electrons near the Jovian exobase, though the reason for their existence was left unspecified. Both of these suggestions can be ruled out because low energy electrons would deposit their energy near the exobase, in conflict with our results.

The characteristics inferred here are consistent with heating by internal gravity waves, and we believe that dissipation of energy carried to the upper atmosphere by internal gravity waves is a likely explanation for the hot Jovian thermosphere. Gravity waves appear to carry the appropriate amount of energy and will deposit that energy in the right pressure regime. Moreover, there is observational evidence for gravity waves at microbar levels. The scintillations seen in the SAO 78505 and earlier occultation data can be interpreted as evidence of internal gravity waves [*Sagan et al.*, 1974]. In fact, *French and Gierasch* [1974] pointed out that the thermal balance in the microbar region is likely to be dominated by gravity waves rather than radiation. A similar situation exists on Neptune. *Roques et al.* [1994] analyze scintillations seen in ground-based occultations of stars by Neptune and demonstrate that if the scintillations are caused by waves, the associated energy deposition rates are larger than radiant sources of energy. *Atreya et al.* [1979] discussed the possibility that gravity wave heating was responsible for the high exospheric temperatures on Jupiter; however, this hypothesis was ruled out because the temperature gradient in the *Festou et al.* [1981] model was too shallow [*Atreya et al.*, 1981]. Thus subsequent work quickly abandoned the wave heating idea [c.f. *Atreya et al.*, 1984; *Strobel et al.*, 1991]. With the new results presented here, gravity wave heating is a strong candidate for the missing heat source.

5. Heating by Gravity Waves

Presumably, gravity waves are generated by meteorological processes in the lower atmosphere. As the waves propagate upward to lower densities, their amplitude grows in proportion to the inverse square root of density. Eventually, the amplitude becomes so large that the temperature gradient in portions of the wave approaches the adiabatic value, $dT/dz = -g/c_p$, which has a value of -1.7 K/km. At this point nonlinear effects can no longer be ignored and the convective instability should generate turbulence. This "breaking" limits any further growth of the wave amplitude. The temperature perturbations in the β -Sco occultation studied by *French and Gierasch* [1974] were characterized by amplitudes of approximately 5 K and vertical wavelengths ranging from several to 20 km. The temperature perturbations derived by *Hubbard et al.* [1995] from the SAO 78505 occultation data appear similar. A wave with an amplitude of 5 K and a vertical wavelength of 18 km has a maximum temperature gradient equal to the adiabatic value; thus, it appears likely the gravity waves near 1μ bar are, in fact, saturated. In their equation [24], *French and Gierasch* [1974] provide an expression for the energy flux carried by gravity waves which depends on the square of the amplitude of the temperature perturbation, the vertical wavenumber, the frequency of the wave, and the state of the background atmosphere. The wave frequency depends on the ratio of the horizontal to vertical wavelengths, which can not be determined from the β -Sco occultation data. *French and Gierasch* note that the temperature perturbations retrieved from the β -Sco data appear to vanish above a density level of 10^{13} cm^{-3} and use this fact to estimate a wave frequency of 10^{-3} s^{-1} . Using this value, along with a vertical wavelength of 20 km and a temperature perturbation of 5 K, implies an energy flux at the 10^{14} cm^{-3} density level of $3.4 \text{ erg cm}^{-2} \text{ s}^{-1}$. Comparing this value to the results of our discussion of the temperature profile above, we see that the energy flux carried by gravity waves is of the order required to explain the thermospheric temperature gradient.

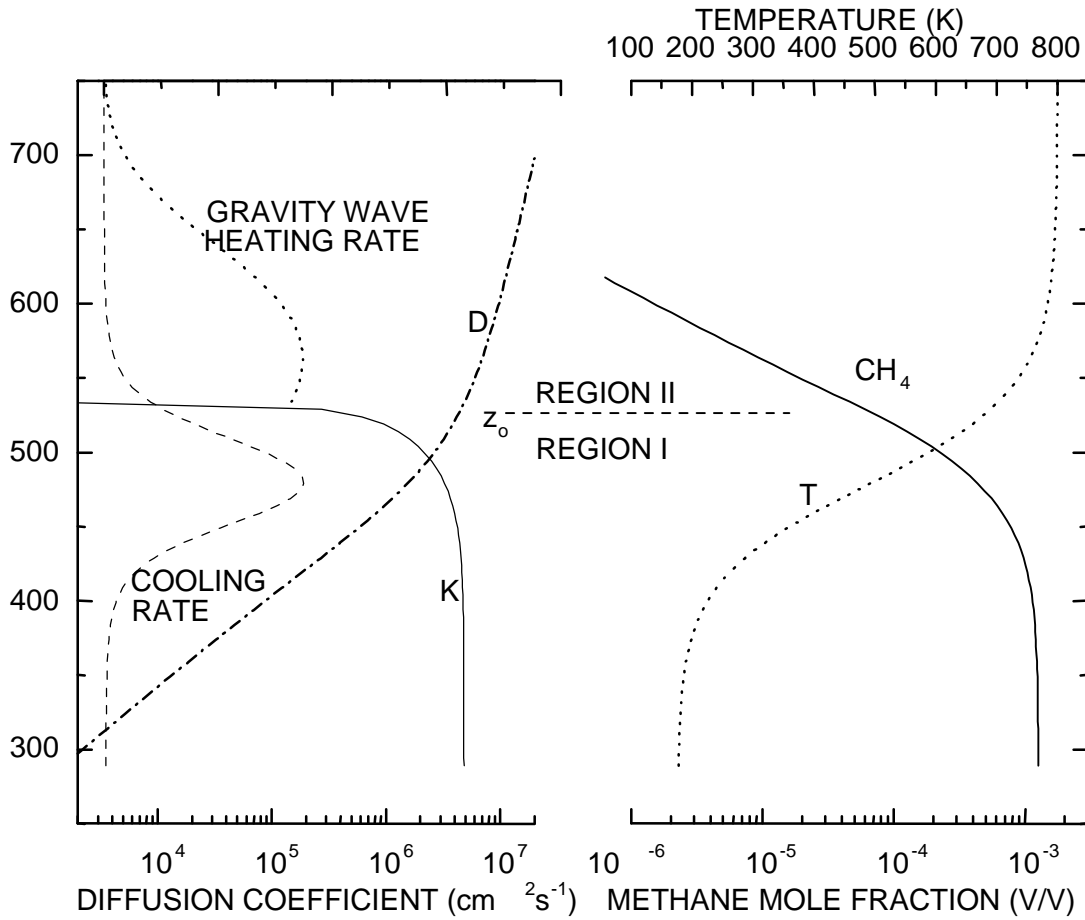


Figure 6. Summary of the physical processes occurring near the CH_4 homopause. The curves shown here are discussed extensively in the text

Gravity waves will also deposit their energy in the pressure regime implied by our analysis of the temperature profile. *French and Gierasch* [1974] argue that the β -Sco observations indicate dissipation of the waves near 1 μbar . They also show that molecular diffusion will cause dissipation of the waves above this pressure level, although this conclusion depends slightly on the ratio of horizontal to vertical wavelengths. For our purposes it is also essential to demonstrate that the gravity wave energy is deposited at altitudes above the region where CH_4 can efficiently radiate away energy. An essential feature of our argument is that gravity waves will be dissipated at roughly 1-2 scale heights above the level where diffusive separation of CH_4 occurs. To investigate this situation we examine the following idealized model, illustrated in Figure 6.

We first review the behavior of the eddy diffusion coefficient caused by gravity wave breaking. At altitudes below z_0 (region I) we assume, following *Linzen* [1981], that eddy viscosity generated by the breaking waves acts to limit wave growth and keeps the amplitude at the saturated level. The amplitude of the wave is given approximately by

$$\mathbf{f} = \mathbf{f}_0 \exp\left[\left(\frac{1}{2H_a} - I_i\right)\lambda_i(z - z_0)\right], \quad (6)$$

where ϕ is any of the wave quantities that vary sinusoidally (the temperature perturbation for example), \mathbf{f}_0 is a constant, H_a is the atmospheric scale height, and λ_i is the imaginary part of the vertical wavenumber [*Holton and Zhu*, 1984]. For the amplitude to remain constant with altitude the imaginary part of the vertical wavenumber must be given by $\lambda_i = 1/2H_a$.

Analysis of the linear wave propagation implies that λ_i is proportional to the viscosity acting on the wave [Linzden, 1981; Schoeberl et al., 1983; Holton and Zhu, 1984]:

$$I_i = \frac{N^3}{k \left| \frac{u}{\mu - c} \right|^4} K_o, \quad (7)$$

where N is the buoyancy frequency, k is the horizontal wavenumber, c is the horizontal wave speed, u is the zonal velocity, and K_o is the viscosity. Both molecular viscosity and eddy viscosity will limit wave growth and $K_o = D + K$, where K is the eddy diffusion coefficient and D is the molecular diffusion coefficient. D varies as the inverse of atmospheric number density ($D = b/n_a$, where b is the binary diffusion coefficient). The other quantities in (7) vary more slowly with altitude; consequently, K must decrease exponentially with increasing altitude in order for λ_i to remain equal to $1/2H_a$. At altitude z_o the molecular diffusion coefficient becomes large enough to limit wave growth without any contribution from eddy viscosity; thus K is negligible at and above altitude z_o . The waves are no longer breaking in region II and no turbulence is generated. The altitude variation of the eddy coefficient implied by these considerations is shown in Figure 6.

The heating rate due to wave dissipation depends on the wave amplitude. D continues to increase above z_o , causing the wave amplitude to decrease below the saturated level and eventually leading to dissipation of all the wave energy. Combining equations (6) and (7) with $D \gg K$ leads to

$$I_i = \frac{1}{2H_a} \frac{p_o}{p}, \quad (8)$$

where p is the atmospheric pressure and p_o its value at z_o . The dependence of λ_i on p arises from the fact that D varies inversely as p . In region II the wave amplitude will decrease according to

$$f = f_o \left(\frac{p_o}{p} \right)^{0.5(1-p/p_o)}, \quad (9)$$

Figure 6 shows an estimate of the heating rate profile based on (9). The heating rate is estimated by taking the altitude derivative of the product of density and wave amplitude squared. The heating rate so estimated is likely to be unreliable below z_o because there are many effects associated with coherent energy propagation by the waves, turbulent transport of energy, etc., that we have ignored. However, our goal is to demonstrate that wave heating extends at least a scale height above z_o , and our formulation is adequate for that purpose. The heating rate is significant for roughly a distance of one scale height above z_o .

The magnitude of the temperature rise caused by wave heating depends on the vertical separation of the heating and cooling regions. Radiative cooling by CH_4 is the primary energy sink. Thus it is essential to determine the CH_4 distribution, which depends on the

eddy diffusion coefficient. The eddy diffusion coefficient implied by the wave saturation hypothesis predicts that diffusive separation of CH_4 will become manifest 1-2 scale heights below z_o . Ignoring for the moment loss due to photolysis, equation [3] for the CH_4 distribution has the following simple solution for the case where $K + D = K_o$ is constant:

$$f = f_\infty \exp\left\{ \left(1 - \frac{m_i}{m_a} \right) \left| \frac{p_o}{p} \right| \right\}, \quad (10)$$

where $f = p/p_o$ is the CH_4 mole fraction, f_∞ is its value deep in the atmosphere, and m_i and m_a represent the mass of a CH_4 molecule and the mean atmospheric molecular mass, respectively. To derive (10), we have also neglected the temperature dependence of the molecular diffusion coefficient and have assumed an eddy Prandtl number of unity. Equation (10) implies that at altitude z_o , diffusive separation has already caused the CH_4 mole fraction to decrease to 0.2% of its value in the lower atmosphere. Including loss due to photolysis or the temperature dependence of D would push the CH_4 distribution to even deeper levels. Moreover, the actual eddy Prandtl number is likely to be larger than unity [Chao and Schoeberl, 1984] and larger values imply a CH_4 density profile that decreases more rapidly than that described by (10). Above z_o the CH_4 density will decrease with altitude according to its own diffusive equilibrium scale height because, according to our assumptions, K is small in this region. The CH_4 distribution described by (10) is shown in Figure 6.

Our analysis demonstrates that gravity waves will be dissipated roughly one scale height above the region where molecular diffusion becomes sufficiently large to damp the waves. Moreover, turbulence generated by the waves weakens near this level and diffusive separation of CH_4 occurs roughly 2-3 scale heights below the heating level. The separation between the heating source and sink implies the presence of a large temperature gradient in the intervening region. This scenario is consistent with our results on the structure of Jupiter's upper atmosphere. The rapid temperature rise demanded by the Liu and Dalgarno [1995] results occurs near 0.3 μbar . Our analysis of the UVS occultation data indicates that diffusive separation of CH_4 occurs at about that level. The scintillations seen in the ground-based occultation data can be interpreted as upward propagating gravity waves at the same pressure level. The gravity waves appear to be saturated, and for plausible values of their frequency they carry an energy flux of the magnitude required to explain the large temperature gradient.

Although the case for gravity wave heating looks promising, there are several reasons to remain cautious. The interpretation of the scintillations seen in the occultation data is not unique. It is possible that these features are not caused by waves but by stationary structures in the Jovian atmosphere. Vertical temperature variations on the order of 5 K could be a

result of the circulation patterns in the Jovian upper atmosphere. If this is the case, then the turbulent mixing in this region must be caused by a process other than the breaking of gravity waves.

Our treatment of the thermal structure and gravity wave energetics has been simplistic because our goal has been to demonstrate that the general characteristics of gravity waves are consistent with the characteristics of the heat source implied by our results on the upper atmospheric structure. Given the success of these exploratory calculations, there are several processes associated with gravity waves that deserve further study. We have neglected radiative damping of the waves. Above the homopause radiative damping can not be important, but in the region where the temperature begins to rise as the CH_4 density begins to drop, radiative damping may have a significant effect on the waves. We have considered energy deposition by the waves only in the region where they are over damped, i.e., where the amplitude is decreasing with altitude. The waves will also deposit energy in the region where they are saturated. Much of this energy may be radiated away by CH_4 , but again there may be significant effects in the transition region where the CH_4 density is beginning to drop. Moreover, the role of breaking gravity waves is not limited to heating; they also affect the thermal balance through the transport of potential temperature and coherent wave energy. Numerical calculations of these effects, though beyond the scope of this paper, are required to quantitatively evaluate these complications. Finally, we emphasize that our analysis is based on *Linzden's* [1981] hypothesis that the eddy coefficient due to breaking gravity waves has the value required to keep the wave amplitude at the saturated level.

6. Summary and Conclusions

The conclusions reached in this study can be summarized as follows:

1. The Jovian atmosphere possesses a strong temperature gradient in the 0.1-1 μbar region: over roughly one decade of pressure the temperature rises from ~ 175 K to ~ 800 K.

2. The temperature rise is coincident with the disappearance of CH_4 from the atmosphere. The maximum temperature gradient occurs at 0.3 μbar , where the CH_4 mole fraction is roughly 10% of its value in the deep atmosphere.

3. The energy flux required to explain the temperature rise is of the order of $1 \text{ erg cm}^{-2} \text{ s}^{-1}$ and the energy must be deposited in the 0.1-1.0 μbar region.

4. The gravity wave interpretation of the scintillations seen in the SAO 78505 occultation data and the β -Sco occultation data implies that the waves carry an energy flux approximately equal to that required to explain the large temperature gradient.

5. Gravity waves will be dissipated in the 0.1-1.0 μbar region, consistent with our inferences on the location of heating from analysis of the temperature profile.

6. Diffusive separation of CH_4 should occur several scale heights below the level where gravity wave energy is deposited. Energy is carried by thermal conduction in the region between the source and the sink, causing the large temperature gradient.

In consideration of conclusions 4-6, dissipation of gravity wave energy appears to be a likely candidate for the energy source responsible for the temperature rise in the Jovian thermosphere.

Several of the conclusions reached in this study can be tested by the Atmospheric Structure Instrument (ASI) on the Galileo probe [*Sieff and Knight*, 1992]. This instrument will determine the vertical structure of the Jovian atmosphere from 0.3 nbar to well below 1 bar with an altitude resolution of 2 km in the microbar region of the atmosphere and an expected precision of 1 K [*Sieff and Knight*, 1992]. Thus the thermal profile in the microbar region will be accurately measured. The probe will enter the atmosphere at a latitude of 6°N , which is similar to the latitudes relevant for the data sets analyzed here. These ASI measurements of the atmospheric structure will directly test the large temperature gradient models proposed here. Moreover, the sensitivity of the ASI is sufficient to measure gravity wave perturbations in the atmosphere. The characteristics of waves discussed here (i.e., temperature perturbations of several kelvins and vertical scales of tens of kilometers) is within the range accessible by ASI measurements. Examination of the characteristics of these waves should more tightly constrain the heating rate due to wave dissipation, providing a better test of our hypothesis that wave heating is responsible for the high thermospheric temperature.

We note that there are other possible sources of heat for the Jovian thermosphere. Energy deposited at high latitudes by the intense aurora on that planet could be transported to low latitudes by thermospheric winds. Quantitative evaluation of this hypothesis is difficult because the auroral energy input is not well determined and the efficiency with which heat can be transported to low latitudes has not been calculated. Also, the aurora on the other giant planets are far weaker than those on Jupiter, yet they all have hot thermospheres, implying the existence of a heating mechanism other than the transport of auroral energy. Joule heating in the ionosphere has also been suggested [*Broadfoot et al.*, 1981; *Nishida and Watanabe*, 1987; *Clarke et al.*, 1987; *Hudson et al.*, 1989] as an energy source for the giant planet thermospheres. As with aurora quantitative evaluation of this hypothesis is difficult. The strength of joule heating depends on the ionospheric structure and the wind fields near in the upper atmosphere. The ionospheric structure on Jupiter is poorly understood, especially in the 0.1-1.0 μbar region, and we know nothing at all about winds in this region. Moreover,

joule heating will act to dissipate the winds, implying that another mechanism must be found to deposit momentum and energy in the appropriate region of the atmosphere.

Our analysis and discussion have concentrated on the Jovian atmosphere. It is important to remember that high thermospheric temperatures occur on Saturn, Uranus, and Neptune as well. Moreover, all these atmospheres have been probed by ground-based stellar occultations, and scintillations are seen in every case. We note that stellar occultation observations of Uranus, though originally interpreted as nearly isothermal at a low temperature, have also been found to be consistent with the large temperature gradients inferred from Voyager UVS occultations [Baron, 1989; Rizk and Hunten 1990]. The model presented here for gravity wave heating and the way in which it is coupled to diffusive separation of CH₄ implies that large temperature gradients should be present near the homopause in all outer planet atmospheres. The process appears to be quite general because the separation between the heating level and the radiative cooling level is primarily a consequence of the mass difference between CH₄ and H₂. Thus an important test of the scenerio outlined here is a reexamination of both the UVS and ground-based occultation data to determine if they are consistent with the presence of large temperature gradients in the 0.1-1.0 μbar region.

Acknowledgments. We are grateful to Melissa McGrath for alerting us to this problem, Weihong Liu and Alex Dalgarno for a preprint of their work prior to publication, Mark Schoeberl for discussions about gravity waves, Steven Miller and Pierre Drossart for help with understanding H₃ emissions, Jay Holberg for assistance with UVS occultation geometry, Michel Festou for digging out his old notes, and Al Sieff for discussions about the Galileo ASI experiment. Also, we would like to thank Randy Gladstone for a helpful reviews of this manuscript. This work was carried out while the first author was a NRC Senior Research Associate at the NASA Ames Research Center.

References

- Atreya, S. K., T. M. Donahue, B. R. Sandel, A. L. Broadfoot, and G. R. Smith, Jovian upper atmospheric temperature measurements by the Voyager 1 UV spectrometer, *Geophys. Res. Lett.*, **6**, 795-798, 1979.
- Atreya, S. K., T. M. Donahue, and M. C. Festou, Jupiter: structure and composition of the upper atmosphere, *Astrophys. J.*, **247**, L43-47, 1981.
- Atreya, S. K., J. H. Waite Jr., T. M. Donahue, A. F. Nagy, and J. C. McConnell, Theory, measurements, and models of the upper atmosphere and ionosphere of Saturn, in *Saturn*, edited by T. Gehrels and M. S. Mathews, pp. 00-00, Univ. of Ariz. Press, Tucson, 1984.
- Baron, R., Occultation astronomy and instrumental studies of the Uranian upper atmosphere, PhD. dissertation, Mass. Inst. of Technol., Cambridge, 1989.
- Broadfoot, A. L., B. R. Sandel, D. E. Shemansky, J. C. McConnell, G. R. Smith, J. B. Holberg, S. K. Atreya, T. M. Donahue, D. F. Strobel, and J.-L. Bertaux, Overview of the Voyager ultraviolet spectrometry results through Jupiter encounter, *J. Geophys. Res.*, **86**, 8259-8284, 1981.
- Broadfoot, A. L., et al., Ultraviolet spectrometer observations of Neptune and Triton, *Science*, **246**, 1459-1466, 1989.
- Chamberlain, J. W., and D. M. Hunten, *Theory of Planetary Atmospheres*, Academic Press, San Diego, Calif., 1987.
- Chao, W. C., and M. R. Schoeberl, On the linear approximation of gravity wave saturation in the mesosphere, *J. Atmos. Sci.*, **41**, 1893-1898, 1984.
- Clarke, J. T., M. K. Hudson, and Y. L. Yung, The excitation of the far ultraviolet electroglow emissions on Uranus, Saturn, and Jupiter, *J. Geophys. Res.*, **92**, 15139-15147, 1987.
- Drossart, P., J.-P. Maillard, J. Caldwell, S. J. Kim, J. K. G. Watson, W. A. Majewski, J. Tennyson, J. H. Waite Jr., and R. Wagener, Detection of H₃ on Jupiter, *Nature*, **340**, 539, 1989.
- Drossart, P., B. Bezaud, S. K. Atreya, J. Bishop, J. H. Waite Jr., and D. Boice, Thermal profiles in the auroral regions of Jupiter, *J. Geophys. Res.*, **98**, 18,803-18,881, 1993.
- Eshleman, V. R., G. L. Tyler, G. E. Wood, G. F. Lindal, J. D. Anderson, G. S. Levy, and T. A. Croft, Radio Science with Voyager at Jupiter: Preliminary profiles of the atmosphere and ionosphere, *Science*, **204**, 976-978, 1979a.
- Eshleman, V. R., G. L. Tyler, G. E. Wood, G. F. Lindal, J. D. Anderson, G. S. Levy, and T. A. Croft, Radio science with Voyager at Jupiter: Initial Voyager 2 results and a Voyager 1 measurement of the Io torus, *Science*, **206**, 959-962, 1979b.
- Feldman, P. D., M. A. McGrath, H. W. Moos, S. T. Durrance, D. F. Strobel, and A. F. Davidson, The spectrum of the Jovian dayglow observed at 3 Å resolution with the Hopkins Ultraviolet Telescope, *Astrophys. J.*, **406**, 279-284, 1993.
- Festou, M. C., S. K. Atreya, T. M. Donahue, B. R. Sandel, D. E. Shemansky, and A. L. Broadfoot, Composition and thermal profiles of the Jovian upper atmosphere determined by the Voyager ultraviolet stellar occultation experiment, *J. Geophys. Res.*, **86**, 5715-5725, 1981.
- Fjeldbo, G., A. Kliore, B. Seidel, B. Sweetnam, and P. Woiceshyn, The Pioneer 11 radio occultation measurements of the Jovian ionosphere, in *Jupiter*, edited by T. Gehrels, pp. 00-00 Univ. of Ariz. Press, Tucson, 1976.
- French, R. G. and P. J. Gierasch, Waves in the Jovian upper atmosphere, *J. Atmos. Sci.*, **31**, 1707-1712, 1974.
- Hanley, H. J. M., R. D. McCarthy, and H. Interemann, The viscosity and thermal conductivity of dilute hydrogen from 150 to 5000 K, *J. Res. Natl. Bur. Stand. U.S. Sect. A.*, **74**, 331-353, 1970.
- Herbert, F., B. R. Sandel, R. V. Yelle, J. B. Holberg, D. E. Shemansky, A. L. Broadfoot, S. K. Atreya, and P. N. Romani, The upper atmosphere of Uranus: EUV occultations observed by Voyager 2, *J. Geophys. Res.*, **83**, 15093-15109, 1987.
- Holton, J. R., and X. Zhu, A further study of gravity wave induced drag and diffusion in the mesosphere, *J. Atmos. Sci.*, **41**, 2653-2662, 1984.
- Hubbard, W. B. and T. C. Van Flandern, The occultation of Beta Scorpil by Jupiter and Io. III. Astrometry, *Astron. J.*, **77**, 65-74, 1972.
- Hubbard, W. B., R. E. Nather, D. S. Evans, F. G. Tull, D. C. Wells, G. W. Van Citters, B. Warner, and P. Vanden Bout, The occultation of Beta Scorpil by Jupiter and Io. I, Jupiter, *Astron. J.*, **77**, 41-59, 1972.
- Hubbard, W. B., V. Hammerle, C. C. Porco, G. H. Rieke, and M. J. Rieke, The occultation of Jupiter by SAO 78505, *Icarus*, **113**, 103-109, 1995.
- Hudson, M. K., J. T. Clarke, and J. A. Warren, Ionospheric dynamo theory for production of far ultraviolet emissions on Uranus, *J. Geophys. Res.*, **94**, 6517-6522, 1989.
- Hunten, D. M., and A. J. Dessler, Soft electrons as a possible heat source for Jupiter's thermosphere, *Planet. Space Sci.*, **25**, 817-821, 1977.
- Hunten, D. M., and J. Ververka, Stellar and spacecraft occultations by Jupiter: a critical review of derived

- temperature profiles, in *Jupiter*, edited by T. Gehrels, pp. 00-00, Univ. of Ariz. Press, Tucson, 1976.
- Lindal, G. F., et al., The atmosphere of Jupiter: An analysis of the Voyager radio occultation experiments, *J. Geophys. Res.*, **86**, 8721-8727, 1981.
- Linzen, R. S., Turbulence and stress owing to gravity wave and tidal breakdown, *J. Geophys. Res.*, **86**, 9707-9714, 1981.
- Liu, W., and A. Dalgarno, The ultraviolet spectrum of the Jovian dayglow, *Astrophys. J.*, in press 1995.
- Livengood, T. A., D. F. Strobel, and H. W. Moos, Long-term study of longitudinal dependence in primary particle precipitation in the north Jovian aurora, *J. Geophys. Res.*, **95**, 10,375-10,388, 1990.
- Marten, A., C. DeBergh, T. Owen, D. Gautier, J. P. Maillard, P. Drossart, B. L. Lutz, and G. S. Orton, Four micron high-resolution spectra of Jupiter in the North Equatorial Belt: $\mathbf{113}$ emissions and the $^{12}\text{C}/^{13}\text{C}$ ratio, *Planet Space Sci.*, **42**, 391-399, 1994.
- McConnell, J. C., J. B. Holberg, G. R. Smith, B. R. Sandel, D. E. Shemansky, and A. L. Broadfoot, A new look at the ionosphere of Jupiter in light of the UVS occultation results, *Planet. Space Sci.*, **30**, 151-167, 1982.
- McConnell, J. C., and T. Majeed, H_3^+ in the Jovian ionosphere, *J. Geophys. Res.*, **92**, 8570-8578, 1987.
- Miller, S., R. D. Joseph, and J. Tennyson, Infrared emissions of H_3^+ in the atmosphere of Jupiter in the 2.1 and 4.0 micron region, *Astrophys. J.*, **360**, L55-L58, 1990.
- Nishida, A., and Y. Watanabe, Joule heating of the Jovian ionosphere by corotation enforcement currents, *J. Geophys. Res.*, **92**, 6083-6090, 1987.
- Rizk, B., and D. M. Hunten, Solar heating of the uranian mesopause by dust of ring origin, *Icarus*, **88**, 429-447, 1990.
- Roques, F., et al., Neptune's upper stratosphere, 1983-1990: Ground-based stellar occultation observations, III, Temperature profiles, *Astron. Astrophys.*, **288**, 985-1011, 1994.
- Sagan, C., J. Ververka, L. Wasserman, J. Elliot, and W. Liller, Jovian atmosphere: Structure and composition between the turbopause and mesopause, *Science*, **184**, 901-903, 1974.
- Schoeberl, M. R., D. F. Strobel, and J. P. Apruzese, A numerical model of gravity wave breaking and stress in the mesosphere, *J. Geophys. Res.*, **88**, 5249-5259, 1983.
- Shemansky, D. E., An explanation for the H Ly α longitudinal asymmetry in the equatorial spectrum of Jupiter: An outcrop of paradoxical energy deposition in the exosphere, *J. Geophys. Res.*, **90**, 2673-2694, 1985.
- Sieff, A. and T. C. D. Knight, The Galileo probe Atmospheric Structure Instrument, *Space Sci. Rev.*, **60**, 203-232, 1992.
- Smith, G. R., and D. M. Hunten, Study of planetary atmospheres by absorptive occultations, *Rev. Geophys.*, **28**, 117-143, 1990.
- Smith, G. R., D. E. Shemansky, J. B. Holberg, A. L. Broadfoot, B. R. Sandel, and J. C. McConnell, Saturn's upper atmosphere from the Voyager 2 EUV solar and stellar occultations, *J. Geophys. Res.*, **88**, 8867-8678, 1983.
- Stevens, M. D., D. F. Strobel, and F. Herbert, An analysis of the Voyager 2 ultraviolet spectrometer occultation data at Uranus: Inferring heat sources and model atmospheres, *Icarus*, **101**, 45-63, 1992.
- Strobel, D. F., and G. R. Smith, On the temperature of the Jovian thermosphere, *J. Atmos. Sci.*, **30**, 718-725, 1973.
- Strobel, D. F., R. V. Yelle, D. E. Shemansky, and S. K. Atreya, The Upper Atmosphere of Uranus, in *Uranus*, edited by J. T. Bergstralh, E. D. Miner, and M. S. Matthews, pp. 00-00, Univ. of Ariz. Press, Tucson, 1991.
- Trafton, L. M., D. F. Lester, and K. L. Thompson, Unidentified emission lines in Jupiter's northern and southern 2 micron aurorae, *Astrophys. J.*, **343**, L73-L76, 1989.
- Vervack, R. J., Jr., B. R. Sandel, G. R. Gladstone, J. C. McConnell, and C. D. Parkinson, Jupiter's He 584 Å dayglow: New results, *Icarus*, **114**, 163-173, 1995.
- Ververka, J., L. H. Wasserman, J. Elliot, C. Sagan, and W. Liller, The occultation of β Scorpii by Jupiter, I, The structure of the Jovian upper atmosphere, *Astron. J.*, **79**, 73-84, 1974.
- Waite, J. H., Jr., T. E. Cravens, J. Kozyra, A. F. Nagy, S. K. Atreya, and R. H. Chen, Electron precipitation and related aeronomy of the Jovian thermosphere and ionosphere, *J. Geophys. Res.*, **88**, 6143-6163, 1983.
- Wallace, L., The thermal structure of Jupiter in the stratosphere and upper troposphere, in *Jupiter*, edited by T. Gehrels, pp. 00-00, Univ. of Ariz. Press, Tucson, Arizona, 1976.
- Wasserman, L. H., and J. Ververka, On the reduction of occultation light curves, *Icarus*, **20**, 322-345, 1973.
- Yelle, R. V., H_2 emissions from the outer planets, *Geophys. Res. Lett.*, **15**, 1145-1148, 1988.
- Yelle, R. V., J. C. McConnell, B. R. Sandel, and A. L. Broadfoot, The dependence of electroglow on the solar flux, *J. Geophys. Res.*, **92**, 15110-15124, 1987.
- Yelle, R. V., F. Herbert, B. R. Sandel, R. J. Vervack Jr., and T. M. Wentzel, The distribution of hydrocarbons in Neptune's upper atmosphere, *Icarus*, **104**, 38-59, 1993.

R. V. Yelle, Astronomy Department, Boston University, 725 Commonwealth Ave., Boston, MA 02215
 L. A. Young, R. Young, L. Pfister, Space Sciences Division, NASA Ames Research Center, Moffett Field, CA 94035
 R. J. Vervack, Jr., B. Sandel, Lunar and Planetary Laboratory, University of Arizona, Tucson, AZ 85721

(Received September 29, 1995; revised October 30, 1995; accepted November 1, 1995)

³Now at Department of Astronomy, Boston University, Boston MA

Copyright 1996 by the American Geophysical Union

Paper number 95JE03384
 0148-0227/96/95JE-03384\$05.00